Pure & Appl. Chem., Vol. 61, No. 11, pp. 1963–1968, 1989.
Printed in Great Britain.

Oxide gels: applications in chromatography and investigations of structure by neutron scattering

John D.F. Ramsay

Chemistry Division, Harwell Laboratory, Oxfordshire, OX11 0RA. U.K.

Abstract – The surface and porous properties of oxide gels which are produced in sol-gel processes are determined by the colloid characteristics of the sols. These characteristics include the particle size, shape and aggregate structure of the sols and their interparticle interaction behaviour. With this insight of sol-gel conversion mechanisms, gels with well defined pore structure have been produced. These have been exploited in high performance gel permeation chromatography for example.

Neutron scattering techniques have been important in establishing the mechanism of sol-gel conversion processes and for obtaining insight into the properties of water in gels with different pore structure.

INTRODUCTION

There has been a long-standing scientific and technological interest in oxide gels which has stemmed from their important surface and porous properties (refs. 1 and 2). These properties have led to extensive applications of gels, as adsorbents, catalysts, chromatographic packings and as precursors for the fabrication of ceramic materials for example. Oxide gels have also proved to be highly suitable model systems, firstly in studies of pore structure formation in solids, and secondly in investigations of the mechanisms of adsorption from both liquid and gas phases. Of particular significance here have been the recent technical development and scientific understanding of sol-gel processes, which have led to considerable control in the pore structure of the oxide gels (ref. 3).

Among a range of techniques which have been used recently to study sol-gel systems, neutron scattering has been particularly important. Thus small angle neutron scattering has provided details of colloid structure and interactions in concentrated sols and the role these play in the development of the pore structure in gels (refs. 4 & 5). Incoherent inelastic and quasielastic neutron scattering techniques have also given new insights into the dynamics and structure of water sorbed in oxide gels (ref. 6). Such investigations have wider significance for our understanding of the perturbation in the properties of water at oxide interfaces and when confined in porous networks of defined structure.

Here we will outline some of these aspects, firstly by illustrating the role of colloid structure in determining the surface and porous properties of oxide gels and demonstrating how this feature has been exploited in the development of chromatographic packings. Secondly, the application of neutron scattering techniques will be illustrated by some recent investigations of silica sol/gel systems.

PORE STRUCTURE FORMATION IN OXIDE GELS

An important feature of sol-gel processes is the control which can be obtained in the surface and porous properties of the resultant oxide gels. This has been achieved from a better understanding of the characteristics of sols (particle size, shape and aggregate structure) and the mechanisms of sol to gel conversion processes. The latter have been established using a range of colloid characterisation techniques, such as light and neutron scattering, as will be outlined later. The influence of sol structure can be illustrated for two contrasting types of sol, containing essentially spherical primary particles, which exist either as discrete colloidal entities or as large aggregates. The conversion of these two types of sol to gels having low and high porosity is depicted schematically in Fig. 1.

Specific surface areas, S_{BET} and pore radii, r_p, of silica and ceria gels obtained from sols containing discrete approximately spherical particles having different diameters, D and density, ρ are shown in Fig. 2. Here S_{BET} decreases with increases in D with an inverse relationship given by $S_{BET} \approx 6/D\rho_{oxide}$. The considerably larger value of ρ_{ceria} (7.1 g cm^{-3}) compared to that of ρ_{SiO_2} (2.2 g cm^{-3}) accords with the relatively small value of 160 m^2 g^{-1} for the surface area, despite the small particle size of 6 nm. In contrast r_p increases linearly with D as shown by the results for silica. (The pore size of the ceria gel (~2 nm) was too low for reliable measurement from the type I nitrogen adsorption isotherm, for reasons previously discussed (ref. 7).) Such behaviour would be expected if the packing arrangement of the particles in the gels was similar, since then the void structure making up the pore space would scale with the particle size. This feature is demonstrated in Fig. 3 by the similarity of porosities, ε, of the different gels which have been derived from the measured pore volumes, V_p, where

$$\varepsilon = \frac{\text{volume of pores}}{\text{total volume}} = \frac{V_p \cdot \rho_{oxide}}{1 + V_p \cdot \rho_{oxide}} \quad (1)$$

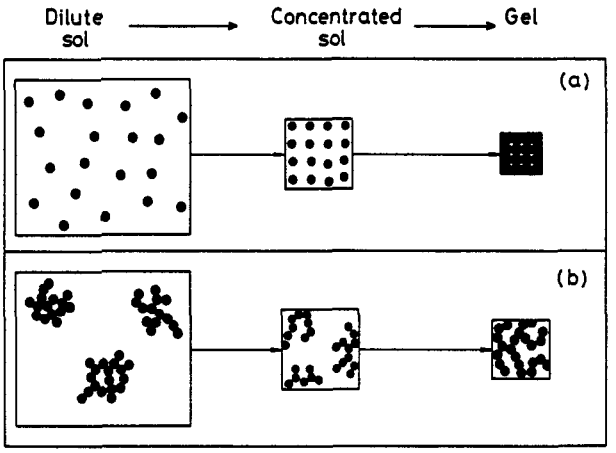

Fig. 1. Diagram depicting the formation of gels of low and high porosity from (a) unaggregated and (b) aggregated sols respectively.

TABLE 1. Properties of regular and random packages of uniform spheres

Type	Z	ε	d/D
Hexagonal	12	0.260	0.155
body centred cubic (bcc)	8	0.320	0.255
simple cubic	6	0.476	0.414
tetrahedral	4	0.660	0.915
"trihedral"*	3	0.815	
random packing+	~7.5	~0.36	0.15-0.55

* N.B. after Heesch and Laves, ref. 8
\+ N.B. after Mason, ref. 15

For the silica gels, values of V_p were in the range of ca. 0.2 to ca. 0.3 $cm^3 g^{-1}$. These porosities are relatively low, indicating an efficient packing of the particles. This is illustrated by the values of ε calculated for regular packings of uniform spheres shown in Table 1, where it is noted that for hexagonal close packing – which is the most efficient, having an ε of 0.26, the interparticle contact or co-ordination number, Z, is 12. Although it is unlikely that in the gels there is a long range regular packing of particles, the low values of ε nevertheless indicate a large interparticle contact number – which on average is probably close to 8 or 9. This aspect will be treated further when the small angle neutron scattering behaviour of concentrated sols and gels are described.

Also shown in Fig. 3 (square symbols) are the corresponding porosities of silica, alumina and titania gels produced from aggregated sols. These are considerably larger, typically between 0.7 and 0.8, which indicates a much more "open" packing where the average contact number is probably close to 3 (ref. 8). This open packing is reflected by the considerably larger values of r_p for the corresponding primary particle size, D (see Fig. 4; N.B. ×10 scale change) compared with the gels derived from non-aggregated sols. The values of S_{BET} are however comparable, which might be expected, because these are determined by the size of the primary particles and are not sensitive to the packing arrangement.

In all the gels described there will be a continuous network of pores of irregular shape formed by the interstices between the particles. The value of r_p, which is effective in the process of capillary condensation will however be determined by the radius, d/2, of the largest sphere which will just fit within the throats (or apertures) interconnecting the cavities of the structure. For regular packings there is a characteristic value of d/D as shown in Table 1. The corresponding values of $2r_p/D$ for the gels of low and high porosity are ~0.21 and ~2.4 respectively, reflecting the markedly different packing geometries in the two classes of gel.

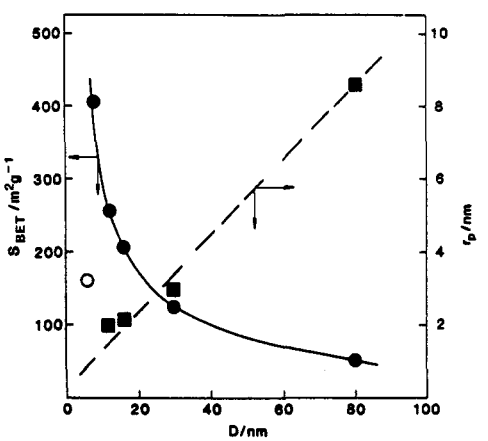

Fig. 2. Specific surface areas, S_{BET}, and mean pore radii, r_p, of silica and ceria gels derived from non-aggregated sols having particle diameters, D.

Symbols ● and ○ refer to S_{BET} of silica and ceria respectively.

■ refers to r_p of silica.

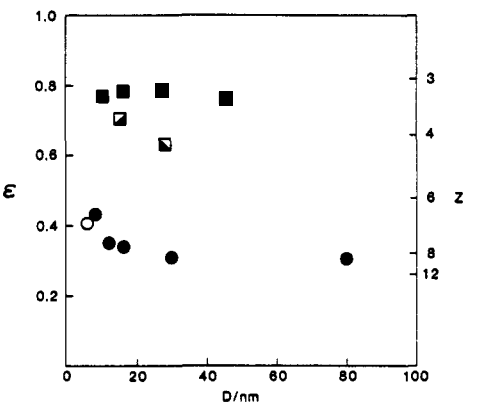

Fig. 3. Porosities, ε, of oxide gels derived from sols having different primary particle sizes, D.

Symbols ● and ○ refer to non-aggregated sols of silica and ceria.

■, ◪ and ◪ refer to aggregated sols of silica, alumina and titania respectively.

Z refers to co-ordination number of regular sphere packing having corresponding porosity.

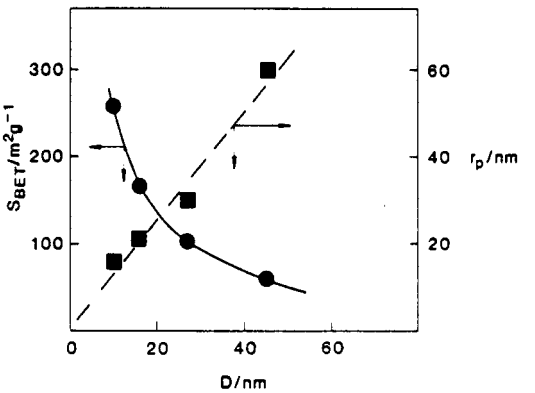

Fig. 4. Specific surface areas, S_{BET}, and mean pore radii, r_p, of silica gels derived from aggregated sols having particle diameters, D.

Symbols ● and ■ refer to S_{BET} and r_p respectively.

PROPERTIES OF GELS IN SIZE EXCLUSION CHROMATOGRAPHY

An important application of oxide gels, such as silica and alumina, has been in high performance liquid chromatography (refs. 9 & 10). Here the gel packings should ideally be produced as small (<20 μm) monosized particles with controlled surface and porous properties (ref. 11). Thus in size exclusion chromatography, the resolution in the separation of macromolecules of different molecular weight is determined by the pore size and uniformity of the gel structure. This feature is illustrated in Fig. 5 showing gel permeation chromatography results for polystyrene standards in tetrahydrofuran. Here a range of polymer standards were separated on six columns, each containing a silica packing of different pore size as previously described. The horizontal lines show the selective permeation range for each silica gel; the upper and lower limits corresponding to total exclusion and total permeation respectively. It will be noted that there is progressive exclusion towards lower MW as the mean pore diameter $\bar{d}_p$, is decreased. The MW of polystyrene at the exclusion limit of each adsorbent can be related to the end-to-end distance, L (nm), of the molecule. For polystyrene in tetrahydrofuran (random coil polymer) this is given by (ref. 12):

$$L = 3.54 \times 10^{-2} M^{0.575} \quad (2)$$

The corresponding plot of $\bar{M}_W$ as a function of L (on the same scale as $\bar{d}_p$) is shown by the broken line in Fig. 5. This demonstrates that the value of L at the exclusion limit of each gel corresponds closely to $\bar{d}_p$. This feature reflects the uniformity of the pore structure for the range of gel packings and gives an insight into the steric exclusion mechanism of the polymers.

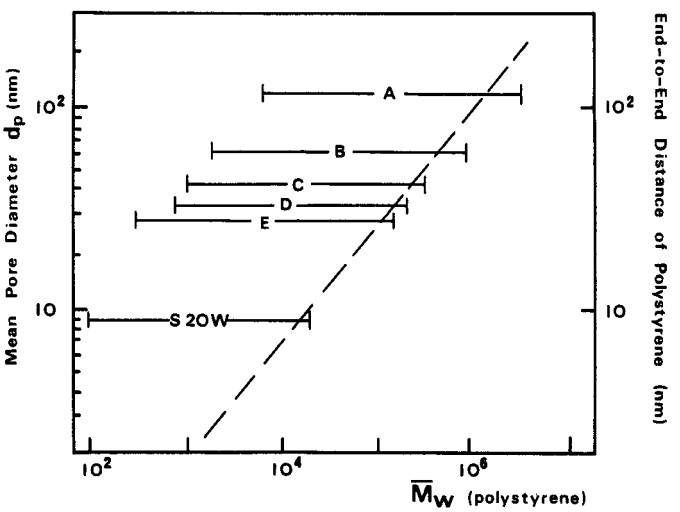

Fig. 5. Selective permeation ranges of polystyrene in silica gel particles with different mean pore diameter. Upper limits correspond to total exclusion and lower limits to total permeation for different gels.

The broken line shows the relationship between L and $\bar{M}_w$ given in eqn. (2).

NEUTRON SCATTERING INVESTIGATIONS OF SOLS AND GELS

Although a range of techniques has been used to study oxide sols and gels the application of neutron scattering is, however, a quite recent development which has led to considerable advances in our understanding of these systems. Here we will firstly illustrate how small angle neutron scattering (SANS) has given details of the colloid structure and interactions in concentrated oxide sols and gels. This has led to new insights into the mechanism of the sol to gel conversion process and highlighted the inter-relationships between sol microstructure and gel pore structure. The second application of neutron scattering has been in the investigation of water in sol-gel systems. Here incoherent inelastic and quasielastic scattering techniques have shown how both the dynamics and structure of water at oxide interfaces may be different from that in the bulk, due to perturbations in the H-bonded structure. It has been possible to investigate such effects systematically where water is confined in well defined porous gel networks as we will briefly describe.

SANS INVESTIGATIONS OF THE SOL TO GEL CONVERSION

The application of SANS is most readily illustrated with reference to sols containing discrete nearly monodispersed spherical particles as depicted in Fig. 1. Such a system is typified by silica sols, and in Fig. 6 SANS results are shown for particles with a diameter of ~16 nm, at progressive stages of concentration until the onset of gel formation. Here the scattered intensity I(Q) is shown as a function of scattering vector, Q, where $Q = 4\pi \sin\theta/\lambda$, for a scattering angle θ and neutron wavelength λ. Although it is not appropriate to discuss these results in detail here, it can be shown, from a detailed analysis of the interference maxima which develop with concentration (refs. 4, 5 & 13), that the sol particles are maintained in a partially ordered arrangement by mutual repulsion forces resulting from the interaction between their charged electrical double layers.

Thus as the sols are concentrated, the interparticle separation is progressively decreased but the relative dispositions of the particles remain similar, as deduced from the particle pair distribution functions, g(r), obtained from scattering data. The latter, which is obtained by a Fourier transform given in (3), defines the probability that the centres of a pair of particles will be separated by a distance r.

$$g(r) = \frac{1}{2\pi^2 n_p} \int_0^\infty [S(Q) - 1]\, Q^2 \frac{\sin Qr}{Qr}\, dr \qquad (3)$$

Here S(Q) is the static structure factor derived from a relationship of the form

$$I(Q) \propto n_p\, P(Q)\, S(Q)$$

where P(Q) is a form factor, defined by the particle size and shape, and n_p is the particle number concentration.

An insight into the structural changes which occur in converting sols into gels can be obtained from the dependence of the equilibrium separation distance, $r_{g(r)_{max}}$, (= r*), on sol concentration c. In general, for these discrete particle systems it is found that the interparticle separation decreases as $c^{1/3}$ and approaches that of the particle diameter, D, as the solid gel is formed. This feature, which is illustrated by results for ceria and silica sols of different particle size in Fig. 7, indicates that there is little change in the relative arrangement of particles when the solid volume fraction is increased by over an order of magnitude. An indication of the arrangement of particles in both sols and gel can also be obtained from g(r). Thus the average number of nearest neighbours, Z, is obtained from the relationship

$$Z = 8\pi n_p \int_0^{r^*} r^2\, g(r)\, dr \qquad (4)$$

Values of Z are in general close to 8 – implying an efficiently packed particle system when the gel is formed. As previously noted (cf. Table 1) this is similar to that for random close packing of spheres where ε is ~0.36 and Z ~7.5 (refs. 14 & 15). The dependence of pore size and specific surface area are also found to correlate with the size of the primary particles packed in such a configuration, as noted earlier.

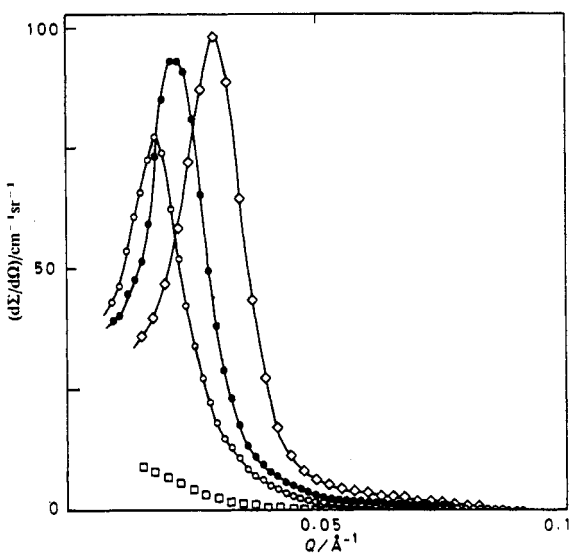

Fig. 6. SANS from silica sols of different concentrations, c: □ 0.014; ○, 0.14; ●, 0.27; and ◇, 0.55 g cm^{-3}.

Particle diameter is ~16 nm.

Scattered intensity is expressed as macroscopic cross-section, $d\Sigma/d\Omega$.

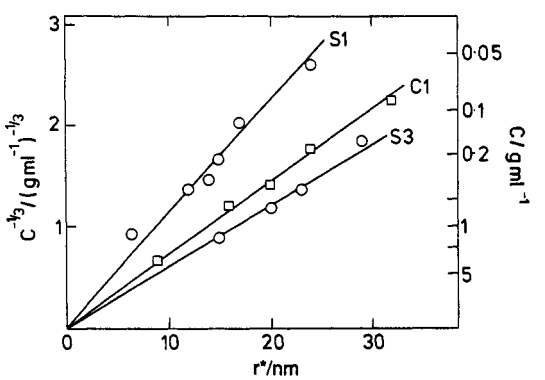

Fig. 7. Dependence of particle separation, r*, on the concentration of sols and gels.

S1, S3 and C1 refer to silica and ceria with particle diameters of 8, 16 and ~6 nm respectively.

STRUCTURE AND DYNAMICS OF WATER IN SOL GEL SYSTEMS

Bulk water under ambient conditions has a markedly H-bonded structure which leads to exceptional liquid properties, as reflected, for example, in its high dielectric constant and diffusion behaviour (ref. 16). It has long been known that this bulk structure may be considerably perturbed in electrolyte solutions and close to charged interfaces, although the nature and range of such effects are still not fully understood. These interfacial perturbation effects have important implications in many areas – colloid interactions, solvation forces, ion and water diffusion in membranes and porous solids, and ion exchange selectivity.

Understanding of the structure and dynamics of water and aqueous solutions has increased rapidly during the past few years. Progress has been particularly significant in neutron scattering studies, where instrumental developments and advances in data treatment and modelling have been considerable (ref. 18). Such investigations have more recently been extended to studies of interfacial water in oxide sol/gel systems as we will outline here. Due to the inherent understanding and control of the microstructure of these systems it has been possible to probe the range and extent of the perturbation of water confined in porous networks in a more systematic way than hitherto. Such studies have included investigations of water (a) at saturation in gels of different pore size (ref. 18), (b) at different uptakes below saturation (ref. 19) and (c) at various stages in the dehydration of sols to gels (refs. 6 & 20). We will only illustrate results for the latter here after outlining the background to the technique.

Incoherent scattering measurements are particularly suitable for the study of hydrogeneous materials such as water because of the large value of the scattering cross section, σ_{inc}, for the proton which dominates that for all other nuclei (ref. 21). This is very significant in situations where other spectroscopic techniques, such as infrared and NMR, are unsuited because of absorption problems. Furthermore because of the high energy resolution which is now attainable in neutron scattering the energy or timescale of dynamic processes which can be studied extends from $\sim 10^{-14}$ s to $\sim 10^{-6}$ s, which is equivalent to a correspondingly large energy transfer range, $\hbar\omega$, extending from $\sim 10^{-1}$ to 10^{-9} eV. Two types of energy transfer process are important in investigations of water structure and dynamics. Firstly those resulting from low energy quantised intermolecular modes in the inelastic range ($\lesssim 10^{-1}$ eV), such as librations, and secondly those resulting from random diffusional motions (translations, rotations) at lower energy ($\lesssim 10^{-3}$ eV) in the quasielastic region. Both of these are dependent on the H-bond structure and therefore are a sensitive reflection of surface perturbation effects.

This feature is illustrated in Fig. 8 by the effect of temperature on the quasielastic scattering from water in a silica gel at two stages of dehydration (~56% and ~73% w/w SiO_2 for (a) and (b) respectively). (Here the silica sol contained particles with a diameter of ~16 nm and eventually gave a gel with pore volume, V_p, of 0.23 $cm^3\ g^{-1}$). In both (a) and (b) the broadening of the quasielastic peaks is due to the diffusional motion of water, which it is noted decreases as the temperature is reduced. However the effects of temperature are different in the two cases: in (a) a gradual narrowing occurs as the temperature is decreased to 273K but thereafter, at 265K, an abrupt decrease occurs giving a peak (iv) which is only slightly broader than the resolution function. This indicates that all the water remains liquid at 273K, but at 265K partial freezing occurs, leaving a small proportion of water in the supercooled state. The latter gives rise to the residual broadening, which is more apparent in the wings of the quasielastic peak.

At the higher silica concentration (73% w/w SiO_2) there are significant differences in behaviour. First the broadening is less at 300 and 278K, indicating a reduction in the rate of diffusion; secondly there is no abrupt decrease in the quasielastic peak width (ix) at 253K which would indicate the onset of freezing. At 233K, peak (x), the quasielastic peak is, however, indistinguishable from the resolution function, which suggests almost complete freezing has now occurred.

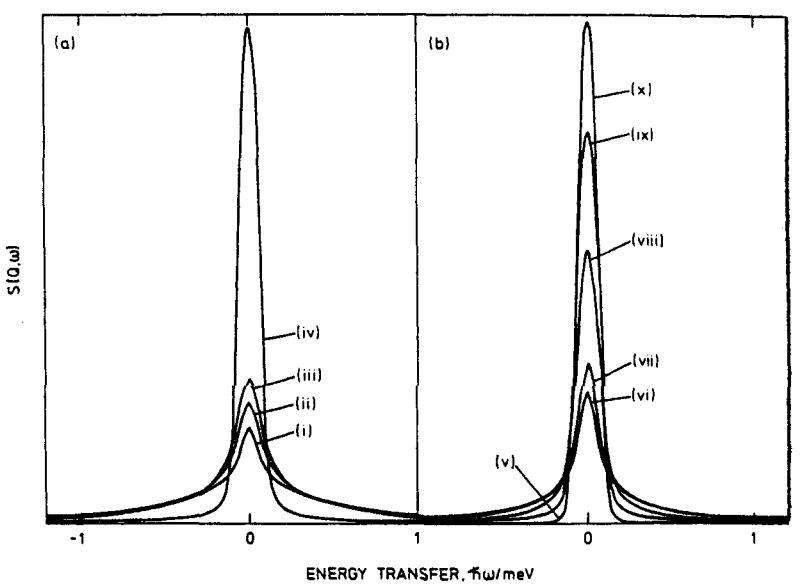

Fig. 8. Evolution of the quasielastic scattering with temperature for water in a silica gel at two stages of dehydration, (a) ~56 and (b) ~73% w/w SiO_2.

Temperatures in (a) are 300, 278, 273 and 265K for (i), (ii), (iii) and (iv). In (b), (v) is the resolution function and temperatures are 300, 278, 268, 253 and 233K corresponding to (vi) to (x) respectively.

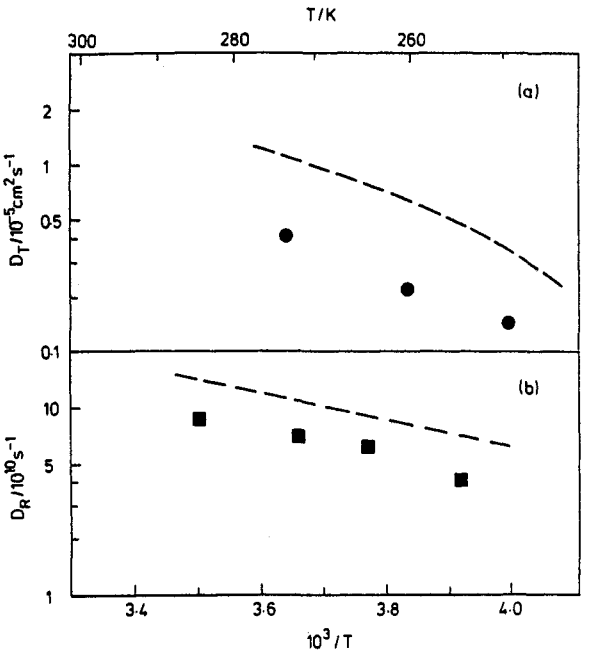

Fig. 9. Dependence of (a) translational diffusion constant, D_T, and (b) rotational diffusion constant, D_R, on temperature for water (0.27 g g^{-1}) in a porous silica gel.

Broken lines show dependence for bulk water.

From a more detailed analysis of quasielastic scattering such as this it is possible to obtain the contributions from translational and rotational diffusion. The results of such an analysis are shown for another silica gel (sol particle diameter ~12 nm), containing 0.27 g g^{-1} H_2O in Fig. 9. Here we note that, compared with the bulk supercooled liquid, the translational diffusion constant, D_T, is reduced more markedly than the rotational diffusion constant D_R. Such a difference may be ascribed to the surface perturbation on the H-bond structure of water, which has a more sensitive effect on translational motion. From a knowledge of the porous structure of these gels, as previously derived from SANS, it has been estimated that such perturbations are insignificant beyond a range of ~6 nm (ref. 6).

Acknowledgements

The work described was undertaken as part of the Underlying Research Programme of the UKAEA. I should like to acknowledge the contributions of many collaborators, in particular Mr. R.G. Avery, Dr. C. Poinsignon and Dr. J.V. Dawkins. Provision of experimental facilities and support at the Institut Laue Langevin, Grenoble are also gratefully acknowledged.

REFERENCES

1. See e.g. A.V. Kiselev, in The Structure and Properties of Porous Materials, p.158, Eds. D.H. Everett and F.S. Stone, Butterworths Scientific Publications, London (1958).
2. B.G. Linsen (Ed.) in Physical and Chemical Aspects of Adsorbents and Catalysts, Academic Press, London (1970).
3. J.D.F. Ramsay, in Better Ceramics through Chemistry III, p.293-304, Eds. C.J. Brinker, D.E. Clarke and D.R. Ulrich, Proc. Mater. Res. Soc., 121, Reno, U.S.A. (1988).
4. J.D.F. Ramsay and B.O. Booth, J. Chem. Soc., Faraday Trans 1, 79, 173-184 (1983).
5. J.D.F. Ramsay, Chem. Soc. Rev., 15, 335-371 (1986).
6. J.D.F. Ramsay and C. Poinsignon, Langmuir, 3, 320-326 (1987).
7. S.J. Gregg and K.S.W. Sing, Adsorption Surface Area and Porosity, p.195, Academic Press (1967).
8. H. Heesch and F. Laves, Z. Krist., A85, 443 (1933).
9. J.H. Knox and M.J. Saleem, J. Chromatog. Sci., 7, 614 (1969).
10. J.J. Kirkland, ibid., 10, 593 (1972).
11. J.V. Dawkins, in Chromatography of Synthetic and Biological Polymers, 1, p.30-56, Ed. R. Epton, Ellis Horwood, Chichester (1978).
12. J.D.F. Ramsay, in Chromatography of Synthetic and Biological Polymers, 1, p.339-343, Ed. R. Epton, Ellis Horwood, Chichester (1978).
13. J. Penfold and J.D.F. Ramsay, J. Chem. Soc., Faraday Trans. 1, 79, 117-125 (1985).
14. J.D. Bernal, Proc. Roy. Soc., A280, 299-322 (1964).
15. G. Mason, Z. Krist., 35, 279 (1971).
16. See e.g. D. Eisenberg and W. Kauzmann, in The Structure and Properties of Water, Oxford Univ. Press, Oxford (1969).
17. See e.g. A.J. Dianoux, Ed., Jour. de Phys., Colloq. C7(1984).
18. J.D.F. Ramsay, H.J. Lauter and J. Tompkinson, J. Phys., C7, 73-79 (1984).
19. J.W. Clark, P.G. Hall, A.J. Pidduck and C.J. Wright, J. Chem. Soc., Faraday Trans. 1, 81, 2067 (1985).
20. C. Poinsignon and J.D.F. Ramsay, J. Chem. Soc., Faraday Trans. 1, 82, 3447-3459 (1986).
21. T. Springer, Quasielastic Neutron Scattering for the Investigation of Diffusive Motions in Solids and Liquids, Springer Tracts in Modern Physics, 64, Springer-Verlag, Berlin (1972).